Design model for square RC columns under compression confined with CFRP

Composites: Part B 57 (2014) 187–198: http://dx.doi.org/10.1016/j.compositesb.2013.09.052

Pedro Faustino[1,2], Carlos Chastre[2], Raquel Paula[3]
[1] *Construction and Environment Section, ESTB – Instituto Politécnico de Setúbal, Portugal*
[2] *Department of Civil Engineering, NOVA University of Lisbon, Portugal*
[3] *Stap – Repair, strengthening and modification of structures, Portugal*

Abstract

The enhancement of the mechanical behaviour of reinforced concrete (RC) columns with regard to axial compression is an up-to-date concern, namely if the strengthening of existing structures is to be considered. In view of this, external confinement with FRP systems has been tested in order to become a feasible technique, since it seems to have important advantages over other systems such as its high strength and stiffness in relation to weight and its improvement of strength and ductility while confining RC columns. Square columns confined with FRP show a more complex interpretation of their behaviour, when compared to circular columns. Accordingly, the present work includes the analysis of two experimental programs regarding axial compression on CFRP confined RC columns: one on circular and square specimens with different corner radii; the other on square specimens with side lengths ranging from medium to large. Based on this, modelling equations are proposed to predict maximum axial load, axial strain and lateral strain, as well as the entire behaviour until failure with curves of axial load-axial strain and axial load-lateral strain. The modelling results show that the analytical curves are in general agreement with the presented experimental curves for a wide range of dimensions.

Key words: A. Carbon fibre, B. Mechanical properties, B. Strength, B. Confinement, C. Analytical modelling,

1. Introduction

Despite being carried out since long ago [1-4], the study of the confinement of reinforced concrete (RC) elements has some important issues that need relevant assessment, namely those regarding columns with square cross-section. Moreover, the option of strengthening with external FRP sheets, which is fairly modelled for RC circular columns [5, 6, 7-10], has not yet a reliable modelling approach for RC square columns.

Differently from circular cross-sections, when square cross-sections are subjected to axial compression the lateral (circumferential) stress is not uniform over the perimeter of the section (Fig. 1), although this stress distribution depends on the detailing of longitudinal and transverse reinforcing steel. Besides the arch effect between hoops, this effect is also present at the level of the section, which means that only a part of the core is confined (Fig. 2).

In the case of external confinement, the effect is similar, encasing as well the cover thickness, and in the particular case of round corners the arch effect is less pronounced and the effective confined area eventually larger. The stress-strain behaviour of columns depends also on the confinement material as regards its properties.

In steel confined concrete, the lateral strain activates the axial stress which, in its turn, increases until the yielding of steel. However, it is likely that yield strength is attained prior to the peak axial stress [11, 12]. Concrete with external passive FRP confinement, in view of the linear elastic behaviour of this composite, presents a different dilatancy performance when compared to concrete with steel confinement [11, 13-16]. With an FRP confinement, while lateral strain increases, the confining circumferential pressure continues to rise until failure.

With respect to the particular case of FRP confinement, contributions of the geometry of the column and the stiffness of the confining material have different influences whether columns' cross section is circular or square [17].

Considering square columns and from the point of view of design, whether the case is of new columns or of existing columns to be strengthened, various models have been proposed for the estimation of confined compressive strength and the resultant strain [18-23].

Saaman et al. [18] proposed a closed bilinear form model for the confinement of concrete with FRP based on Richard and Abbott's equation [24] for both axial and lateral strains. It defines an empirical equation for the peak stress and corresponding axial strain and it considers that the confining lateral stress is obtained from the failure tension value of the FRP. It does not take into account the confinement contribution given by steel hoops on RC columns.

Campione and Miraglia [21] presented a bilinear model for square columns only. The peak axial stress is predicted considering a confinement effectiveness coefficient on Richart et al.'s equation, obtained experimentally. The failure lateral stress is obtained using an expression that considers the effect of corner radius and where there is also a reduction factor experimentally calibrated. The confinement contribution given by steel hoops on RC columns is not regarded as it is not the axial load – lateral strain behaviour.

The model of Lam and Teng [22] is also dependant of the calculus of peak axial stress and related axial strain before applying their own equations that allow creating the stress-strain curve. This model uses as well calibrated coefficients to consider the confinement effectiveness. The authors assume that the effective lateral failure strain is only a portion of the FRP failure strain. Steel hoops are also not regarded as a contribution to confinement.

The model proposed by Manfredi and Realfonzo [19] is based on Spoelstra and Monti [13] with specific modifications in order to consider the effect of geometry on the confinement of square sections. These adjustments include an efficacy factor and a reduction factor when calculating the lateral stress of confinement. It is therefore an incremental model where there is compatibility of lateral dilatancy between concrete and the confining FRP, based on Mander et al. formulation for the stress-strain relation and on Pantazopoulou and Mills [25] for the axial-to-lateral relation. This model does not explicitly account the confinement contribution given by steel hoops on RC columns.

Wang and Restrepo [20] have considered that only part of the area is confined by an effective confining pressure; in which the remaining area is assumed to be unconfined. To calculate the axial strength, they have considered Mander et al.'s model based on Popovics [26] to take into account the stress contributions of both the effectively confined and unconfined areas. The authors account for the contribution of reinforcing steel although an axial-to-lateral relation is not explicit and neither the stress-lateral strain is presented.

The model proposed by Lee [23] is also dilatancy-based. However, the strain–softening of unconfined concrete is modelled through a modified version of Pantazopoulou and Mills [25]. The author proposes that the concrete strength developed from triaxial tests is a better representation of the actual mechanical response of confined concrete and changes the Pantazopoulou and Mills' equations accordingly. The unconfined and confined areas in the cross-section are quantified separately. This model does not explicitly account the confinement contribution given by steel hoops on RC columns.

Given the fact that several characteristics of confined square columns are not yet enlightened, the purpose of the present work is to contribute for a better understanding of the behaviour of square RC columns confined with CFRP. This is done by assessing the existing experimental data, and governing parameters, and to provide simple though reliable tools for the modelling of corresponding behaviour.

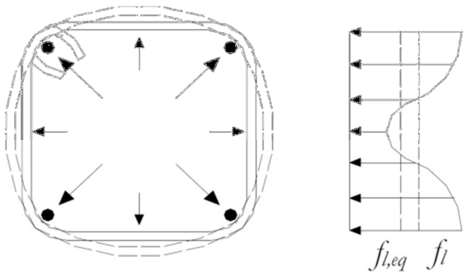

Fig. 1. Lateral stress f_l and equivalent lateral stress $f_{l,eq}$ distributions in RC square cross-section (adapted from Saatcioglu and Razvi [27]).

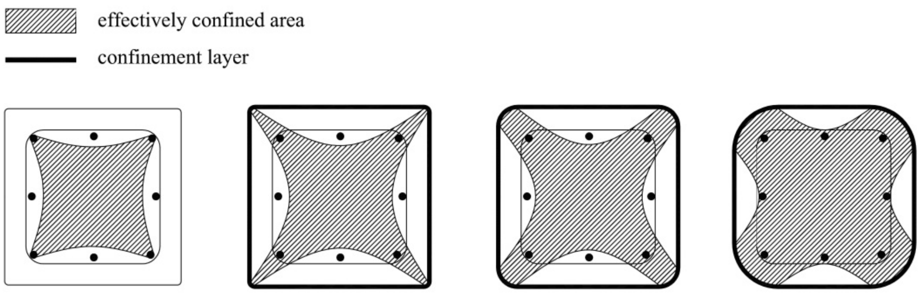

Fig. 2. Effective confined concrete in square RC cross-section with and without external strengthening.

2. Experimental data

2.1. Description of Tested Columns

So that a reliable model for the behaviour of CFRP confined square columns can be proposed, two sets of experimental data with different characteristics were chosen.

The first part of the experimental data aimed at studying the behaviour of concrete columns confined with carbon fibre composites (CFRP) included a research program that was developed at NOVA University of Lisbon (uNL) by Paula [28]. Herein, the purpose is to analyse the influence of geometry concerning the corner radius. This experimental program included 18 monotonic axial tests on short RC columns with 0.75 m height (Table 1), of which 6 have circular cross section (CNR – non-confined and CC – confined with CFRP) with Ø150 mm and 12 have square cross section (QR*x*NR*x* – non-confined and QR*x*C*x* – confined with CFRP) of 150x150 mm2 with different corner radii: 0 mm; 20 mm; 38 mm. The details of the reinforcing steel are shown in Fig. 3. For the columns confinement the used composites were unidirectional CFRP sheets, whose properties are shown in Table 3. The superposed dimension of CFRP wraps was of approximately 300 mm.

The second part of the experimental data was obtained from Rocca [29]. The purpose is to examine the behaviour of columns with different real scale dimensions. This included 11 square RC columns confined with unidirectional CFRP sheets and subjected to axial compression with greater dimensions: square cross sections of 324x324 mm2 (0.69 m height); 457x457 mm2 (1.02 m height); 648x648 mm2 (1.37 m height); 914x914 mm2 (1.98 m height) – Table 2.

For all analysed columns the longitudinal reinforcement ratio ρ_L, the volumetric ratio of transverse reinforcing steel ρ_v and the volumetric ratio of CFRP reinforcement ρ_f are shown in Tables 1 and 2.

Table 1 - Geometrical section properties and detailing of columns tested at uNL by Paula [28]

Column	B (mm)	R (mm)	R/B	H (mm)	Long. steel reinforce.	Transv. steel reinforce.	$t_{f\,CFRP}$ (mm)	$n_{f\,CFRP}$ (mm)	ρ_L (%)	ρ_v (%)	ρ_f (%)
CNR1	150	-	-	731	8Ø6	Ø3//100	-	-	1.00	0.22	-
CNR2	150	-	-	730	8Ø6	Ø3//100	-	-	1.00	0.22	-
CNR3	150	-	-	730	8Ø6	Ø3//100	-	-	1.00	0.22	-
CC1	150	-	-	750	8Ø6	Ø3//100	0.176	2	1.00	0.22	0.94
CC2	150	-	-	750	8Ø6	Ø3//100	0.176	2	1.00	0.22	0.94

CC3	150	-	-	750	8Ø6	Ø3//100	0.176	2	1.00	0.22	0.94
QR1NR1	150	0	0	750	8Ø6	Ø3//100	-	-	1.00	0.11	-
QR1NR2	150	0	0	750	8Ø6	Ø3//100	-	-	1.00	0.11	-
QR1NR3	150	0	0	750	8Ø6	Ø3//100	-	-	1.00	0.11	-
QR1C1	150	0	0	750	8Ø6	Ø3//100	0.176	2	1.00	0.11	0.94
QR1C2	150	0	0	750	8Ø6	Ø3//100	0.176	2	1.00	0.11	0.94
QR1C3	150	0	0	750	8Ø6	Ø3//100	0.176	2	1.00	0.11	0.94
QR2C1	151	20	0.132	750	8Ø6	Ø3//100	0.176	2	1.00	0.11	0.89
QR2C2	151	20	0.132	750	8Ø6	Ø3//100	0.176	2	1.00	0.11	0.89
QR2C3	151	20	0.132	750	8Ø6	Ø3//100	0.176	2	1.00	0.11	0.89
QR3C1	154	38	0.247	750	8Ø6	Ø3//100	0.176	2	1.00	0.11	0.85
QR3C2	154	38	0.247	750	8Ø6	Ø3//100	0.176	2	1.00	0.11	0.85
QR3C3	154	38	0.247	750	8Ø6	Ø3//100	0.176	2	1.00	0.11	0.85

B is the diameter for circular columns and the side length for square columns; R is the corner radius of the square cross section; H is the height of the columns; t_f is the thickness of each ply of CFRP sheet; n_f is the number of used CFRP sheet plies; ρ_L is the longitudinal reinforcement ratio; ρ_v is the volumetric ratio of transverse reinforcing steel and ρ_f the volumetric ratio of CFRP confinement.

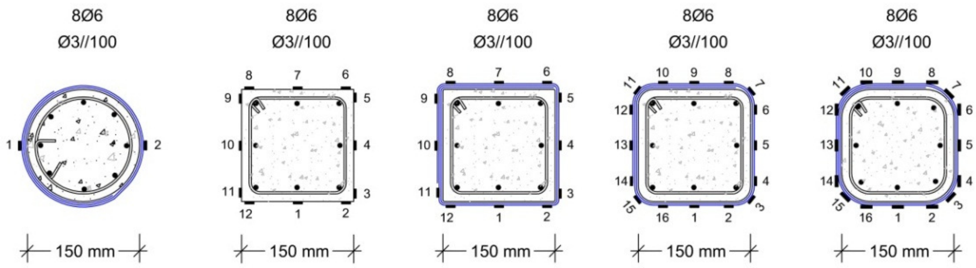

Fig. 3. Reinforcement and details of circular and square columns and gauges position tested at uNL by Paula [28]

Table 2 - Geometrical section properties and detailing of columns tested by Rocca [29]

Column	B (mm)	R (mm)	R/B	H (mm)	$t_{f\,CFRP}$ (mm)	$n_{f\,CFRP}$ (mm)	ρ_L (%)	ρ_v (%)	ρ_f (%)
C1	457	30.5	0.067	1016	-		1.48	0.21	-
C2	457	30.5	0.067	1016	0.168	4 *	1.48	0.21	0.58
C3	457	30.5	0.067	1016	0.168	2 *	1.48	0.21	0.29
D1	648	30.5	0.047	1372	-		1.48	0.21	-
D2	648	30.5	0.047	1372	0.168	5 *	1.48	0.21	0.52
D3	648	30.5	0.047	1372	0.168	2 *	1.48	0.21	0.21
E1	324	30.5	0.094	686	-		1.53	0.45	-
E2	324	30.5	0.094	686	0.168	2 *	1.53	0.45	0.41
E3	324	30.5	0.094	686	0.168	2.5 *	1.53	0.45	0.53
G1	914	30.5	0.033	1981	-		1.50	0.17	-
G2	914	30.5	0.033	1981	0.168	8 *	1.50	0.17	0.58

The longitudinal and transverse steel reinforcement is not available in the study [29]

*obtained from the volumetric ratio of CFRP confinement ρ_f

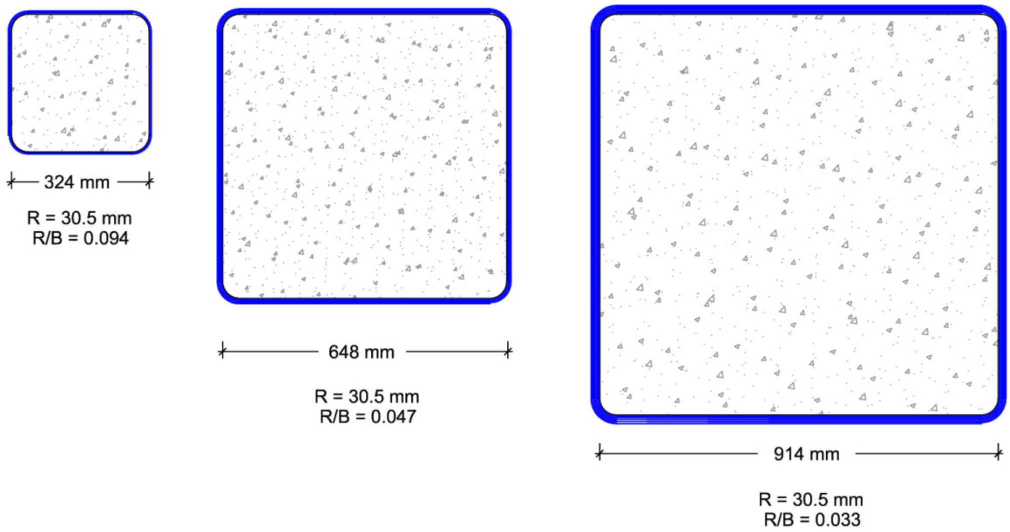

Fig. 4. Geometry of tested square columns by Rocca [29]

2.2. Testing Setup

Axial tests by Paula [28] were carried out with a 5000kN press at uNL and corresponding testing data obtained from UPM100 Data Logger. Tests were carried out controlling the displacement using a speed of 0.01mm/s and stopped after failure until 150kN of force were reached. Three vertical displacement transducers (TML-CDP100) and various strain gauges (120 Ω), were positioned around the column in order to measure the columns vertical and lateral strains (Fig. 3).

The instrumentation in all the specimens by Rocca [29] consisted of electrical strain gauges located on the longitudinal and transverse reinforcing steel, and on the FRP sheet at critical locations (corner areas and mid-distance on each face of the non-circular specimens) along the perimeter of the cross-section on the central region of the strengthened specimens. External sensors to measure axial deformation were also used: potentiometers or LVDTs were affixed to the faces of the columns at about mid-height. The largest columns SCG1 and SCG2 were tested at NIST, while the remaining columns were tested at UCSD. Both laboratories are capable of applying an axial compressive force of 53 000 kN.

2.3. Material Characterization

The characterization of used materials followed the standards [30-32]. The mean concrete compressive strength at the age of concrete columns tests, was f_{c0} =34.6 MPa. The results of yield strength of the reinforcing steel samples was of 587 MPa for Ø6 (longitudinal steel) and 500 MPa for Ø3 (transverse steel).

Tension tests carried out at uNL on carbon fibers sheets resulted in E_f =217 GPa, f_{fu} =3983 MPa and the ultimate strain ε_{fu} of 1.55% for specimens with 2 plies with t_f =0.176 mm each.

Table 3 summarizes the results of material characterization of the materials tested at uNL by Paula [28] and those obtained from Rocca [29].

Table 3 - Materials properties

	Concrete	Long. steel	Transverse steel	CFRP		
Source	f_{c0} (MPa)	f_y (MPa)	f_{wy} (MPa)	E_f (GPa)	f_f (MPa)	ε_{fu} (%)
Paula [24]	34.6	587	500	217	3983	1.55
Rocca [25]	30.5	446	450	291	2668	0.93

3. Tests results

As discussed previously, the confinement effect is affected by columns' cross-section geometry. In the case of circular RC columns the confined concrete is in the core region and the unconfined concrete in the cover region [33]. For circular RC columns, when the strengthening includes confinement with CFRP sheets all concrete cross-section is confined together with the reinforcing steel, acting as a whole until failure of the CFRP confinement. As regards square RC columns only part of the core inside the steel hoops is confined due to the geometric effect of corners [27, 33] and the performance of external confinement with CFRP is thus in the same way influenced by this effect which leads to less efficiency when compared to circular columns.

In view of the previous, the option for the displayed set of columns [28, 29] relies on the available testing data and the geometrical characteristics which include the variation of R/B (corner radius / side length) and the large range of cross-section dimensions (150x150 to 914x914 mm^2).

Throughout compression tests two slopes are developed. Each slope defines a branch and the switch between the two branches represents concrete cracking that is followed by the activation of the confining materials – steel hoops and CFRP sheets. The greater the confinement the higher the slop of the second branch is.

Considering all parameters the same, columns with circular cross section are more efficiently confined and hence present greater second branch slops. In square columns confinement shows less efficiency the sharper the edges are.

3.1 **Tests by Paula** [28]

Table 4 summarizes the test results of axial compression on non-confined and confined RC columns tested by Paula [28]. It is shown that on the whole there is an increase of strength and ductility for both circular and square RC columns confined with CFRP when compared to non-confined RC columns.

For each implemented test, the diagram includes two curves, one with the axial load versus axial strain (ε_c) and another with the axial load versus lateral strain (ε_l). The corresponding load-strain behaviour and failure modes of some of the columns are shown in Fig. 5.

Displacement transducers allowed the reading of the axial strain, while the lateral strains were measured from strain gauges positioned at the specimen's contour. The lateral strain indicated in Fig. 5 corresponds to the reading of gauges placed at the mid-height of each column where higher values of lateral strain would be expected. The chosen gauges for each column were those with higher lateral strain value and in all cases the gauges with highest measurements corresponded to those placed at the corners. These were therefore outside the overlapping zone, which might affect the interpretation of results' relevance [34,35]. According to an experimental work by Lam and Teng [36] the lateral strain values measured in the overlapping zones are in general lower than those of the remaining zones.

Table 4 – Tests results of axial compression in circular and square RC columns by Paula [28]

Column	*CR*	*MCR*	F_{cc} (kN)	F_{cc} / F_{cN}	ε_{cc} (%)	F_{cu} (kN)	ε_{cu} (%)	ε_{cu} / ε_{cuN}	ε_{lu} (%)
CNR1	-	-	491	-	0.203	-	0.203	-	-
CNR2	-	-	491	-	0.188	-	0.188	-	-
CNR3	-	-	491	-	0.236	-	0.236	-	-
CC1	0.50	-	1838	3.7	2.437	-	2.437	11.7	1.446
CC2	0.50	-	1843	3.8	2.532	-	2.532	12.1	NA
CC3	0.50	-	1804	3.7	2.684	-	2.684	12.8	1.191
QR1NR1	-	-	621	-	0.204	-	0.204	-	-
QR1NR2	-	-	641	-	0.217	-	0.217	-	-
QR1NR3	-	-	563	-	0.253	-	0.253	-	-
QR1C1	-	0.01	760	1.3	0.686	745	2.940	13.1	1.151
QR1C2	-	0.01	751	1.2	0.684	713	2.193	9.8	0.389
QR1C3	-	0.01	787	1.3	0.364	742	2.185	9.7	0.155
QR2C1	-	0.13	1130	1.9	2.649	-	2.649	11.8	1.631
QR2C2	-	0.13	1267	2.1	2.958	-	2.958	13.2	1.250
QR2C3	-	0.13	1184	2.0	2.742	-	2.742	12.2	1.581

QR2C1	-	0.24	1380	2.3	1.553	-	1.553	6.9	0.870
QR2C2	-	0.24	1454	2.4	2.448	-	2.448	10.9	1.683
QR2C3	-	0.24	1416	2.3	1.944	-	1.944	8.7	1.140

For circular columns the confinement ratio is $CR = \left(\frac{f_{lf}}{f_{c0}}\right)$; MCR is the modified confinement ratio defined by Mirmiran et al. [37] for square columns in order to account for the sharpness of the edges: $MCR = \frac{2R}{B}\left(\frac{f_{lf}}{f_{c0}}\right)$ where $f_{lf} = \frac{2\,n_f\,t_f\,f_f}{B}$; F_{cc} is the maximum axial load of each column; F_{cN} is the mean value of F_{cc} of the set of 3 RC columns without CFRP confinement; ε_{cc} is the axial strain at F_{cc} of each column; F_{cu} is the ultimate axial load of each column; ε_{cu} is the ultimate axial strain at F_{cc} of each column; ε_{cuN} is the mean value of ε_{cu} of the set of 3 columns without CFRP confinement; ε_{lu} is the higher value of lateral strain at which failure of the CFRP occurred.

NA – not available;

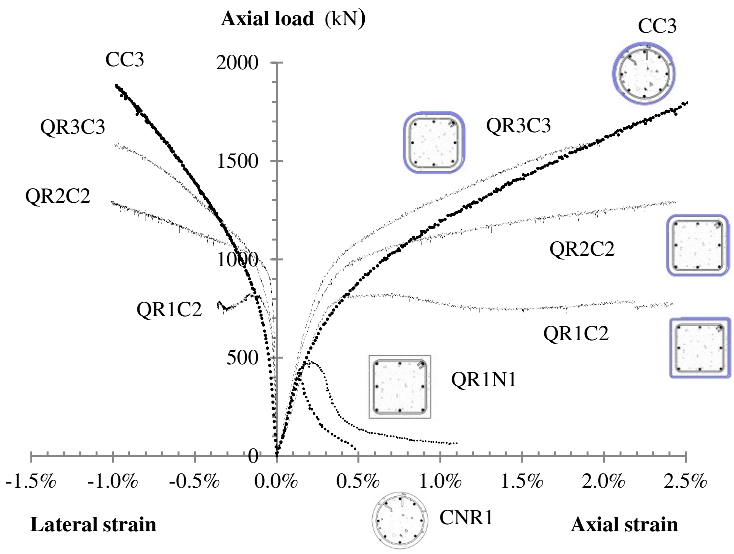

Fig. 5. Axial load vs. strain curves of RC columns with and without CFRP confinement by Paula [28].

The analysis of Table 4 allows the comparison of the performance of all columns as regards strength and ductility. For the circular columns the mean increase in strength between RC specimens (CNR) and those confined with 2 layers of CFRP (CC) is of 3.7 times (491 to 1828 kN), while for the strain at peak load the increase was of 12.2 times (0.209% to 2.550%). For the square columns without round corners (QR1C), in comparison with the square unconfined RC columns (QR1NR), the same relation shows an increase in strength of 1.3 times (608 to 766 kN) and an increase in the ultimate strain of 9.8 times (0.225% to 2.189%). The confined square columns with corner radius R=20mm (QR2C) present mean values of strength 2.0 times higher (608 to 1194kN) than those of unconfined RC columns and mean values of ultimate strain 12.4 times higher (0.225% to 2.784%). As to the confined square columns with corner radius R=38mm (QR3C) the increase in strength is of 2.3 times (608 to 1417kN) and 8.8 times (0.225% to 1.982%) for ultimate strain.

From Fig. 5 it can be seen that for square columns there is no significant difference in the first branch either for the load – axial strain relation or the load – lateral strain relation. It is from the second branch of each tested column that the main difference in the behaviour is verified, where the slope represents the stiffness E_2 of the column after concrete cracking and the activation of the confinement – steel hoops and CFRP. It is clear that for circular columns the slope of the second branch is higher which leads to greater values of strength and stiffness and therefore it shows a more efficient confinement. Despite the slight difference in the CFRP volumetric ratio between all strengthened columns (ρ_f varies from 0.94% to 0.85%), it is clear (fig. 5) that for circular columns the confinement is more effective, which due to the uniformity of lateral stress distribution. . Columns with sharper corners have more pronounced a strain softening with lower slope ($E_2 \approx 0$ for R=0) which means with no increase in strength beyond the first branch. However, the higher the corner radii presented by the square columns the closer their performance ($E_{2,mean}$=5.0GPa for R=20mm and $E_{2,mean}$=15.3GPa for R=38mm) gets to that of circular cross-section ($E_{2,mean}$=23.7GPa).

3.2 **Tests by Rocca** [25]

Table 5 presents the experimental results of all RC square columns confined with CFRP tested by Rocca [29]. Figs. 6 and 7 show the curves corresponding to three of these columns with cross sections of 324x324 mm^2, 648x648 mm^2 and 914x914 mm^2, all with corner radius R=30.5 mm. The behaviour is similar for the three columns (D2, E3 and G2) with strain softening, which means decreasing slope in the second branch (E_2 = - 1.77GPa for D2, E_2 = - 0.22GPa for E3, E_2 = - 0.49GPa for G2). The ultimate axial strain values vary between 1.86 and 6.01 times the ultimate axial strain of unconfined RC columns. Concerning strength there is an increase, where peak strength varies from 1.10 to 1.54 times the same parameter for unconfined RC columns. As to lateral strain, the results present ultimate lateral strain values of 0.68% to 0.74%, that is, respectively, between 73% and 91% of the CFRP failure strain - ε_{fu} = 0.93% (Table 3).

Table 5 – Tests results of axial compression in square RC columns by Rocca [29]

Column	*MCR*	F_{cc} (kN)	F_{cc} / F_{cN}	ε_{cc} (%)	F_{cu} (kN)	ε_{cu} (%)	ε_{cu} / ε_{cuN} *	ε_{lu} (%)
C1	-	6741	-	0.24	NA	0.24	-	-
C2	0.031	7348	1.09	0.47	6242	1.08	4.52	0.58
C3	0.013	7078	1.05	0.27	5201	0.40	1.67	0.62
D1	-	13265	-	0.25	NA	0.29	-	-
D2	0.019	15387	1.16	0.32	10687	0.68	2.34	0.74
D3	0.006	14060	1.06	0.31	9639	0.42	1.44	0.71
E1	-	2673	-	0.15	NA	0.16	-	-
E2	0.022	3983	1.49	0.23	3230	0.27	1.69	0.55
E3	0.031	4116	1.54	0.28	3438	0.96	6.01	0.68
G1	-	28177	-	0.26	NA	0.52	-	-
G2	0.016	30995	1.10	0.33	21700	0.97	1.86	0.67

NA – not available;

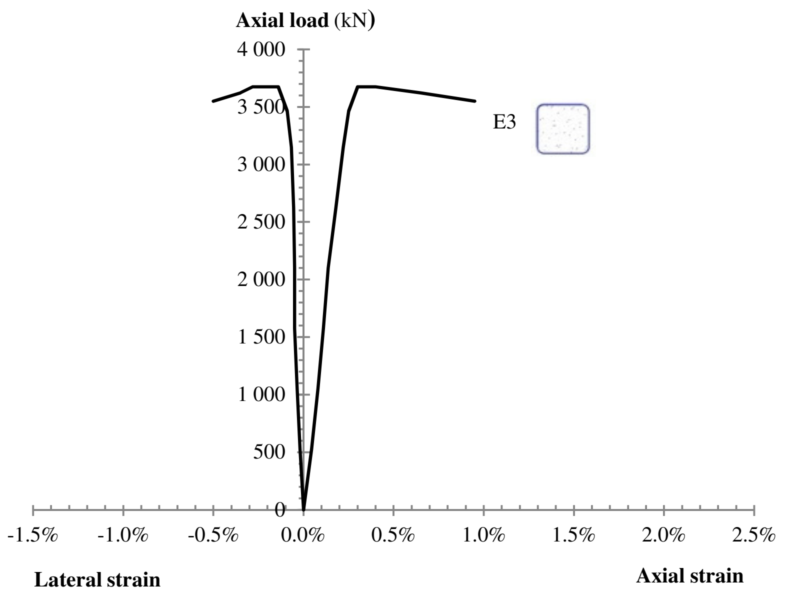

Fig. 6. Axial load vs. strain curves of square RC columns 324x324 mm^2 with CFRP confinement by Rocca [29].

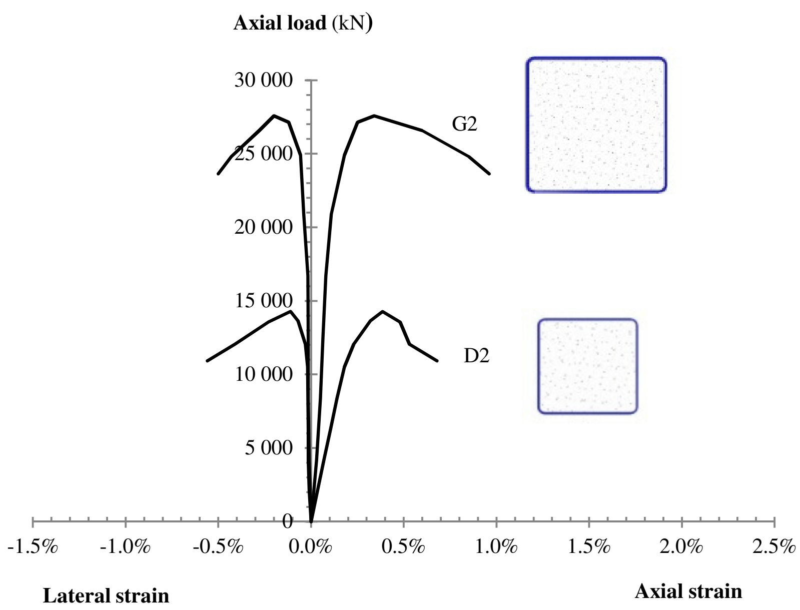

Fig. 7. Axial load vs. strain curves of square RC columns 648x648 mm^2 and 914x914 mm^2 with CFRP confinement by Rocca [29].

4. Numerical model for square RC columns confined with CFRP under axial compressive load

The present section presents two different procedures regarding the behaviour of square columns under compression. The first is related to the use of equations for the calculation of governing parameters, based on the experimental tests, and the second concerns the stress-strain model for confined concrete under compression and the subsequent axial load versus strain of the RC column.

The first procedure consists of merely applying the equations in order to obtain the peak compressive stress f_{cc}, the column's maximum axial load N_{cc}, the axial strain ε_{cc} at peak stress and lateral strain ε_{lu} at rupture. In the second procedure, a model is proposed in order to build the curves of: confined stress f_c as function of axial strain ε_c and lateral strain ε_l and corresponding axial load N_c also as function of axial strain ε_c and lateral strain ε_l. The results of the first procedures establish the limits for the curves obtained in the second procedure.

The validation of the proposed model for the simulation of the behaviour of large-scale square RC columns confined with CFRP under axial compression was carried out with resort to experimental data of Paula [28] and Rocca [29] shown in the previous section. The choice of both these research works relies on the broad variety of parameters such as: i) corner ratio: R/B (from 0.033 to 0.247); ii) columns' cross-section dimensions: B (150, 324, 457, 648 and 914mm); iii) longitudinal reinforcing steel ratio: ρ_L (1% and 1.5%); iv) transverse steel volumetric ratio: ρ_v (0.11% to 0.45%) and v) CFRP volumetric ratio: ρ_f (0.21% to 0.94%). The proposed model is used assuming that the whole column's section is under compression.

The governing parameters necessary for the simulation of the behaviour of columns under axial compression are defined using Eqs. (2), (8), (9) and (10) which includes calculating; the confined concrete stress f_{cc}; the axial strain ε_{cc} at peak stress; lateral ultimate strain ε_{lu} and the columns' maximum axial load N_{cc}. The input initial data for the calculus of the previous parameters are geometrical and strength characteristic of the concrete columns - the dimensions of the square cross-section BxB; the corner radius R; the concrete unconfined stress f_{c0} and strain ε_{c0} – the characteristics of the CFRP confining sheet – thickness t_{ply}, Young modulus E_f and failure strain ε_{fu} – and the characteristics of the reinforcing steel – steel cross sections A_s and A_{sw} or the longitudinal and transverse ratios, the Young modulus E_s, the yielding strengths f_y, and f_{yw}, the hoop dimensions d_s and the spacing between hoops s

4.1. Proposed equations for the governing parameters of columns' behaviour under axial compression

For circular columns the peak stress of the confined concrete f_{cc} can be associated with the unconfined compressive strength f_{c0} and the lateral confining pressure f_{lu} using Eq. (1):

$$f_{cc} = f_{c0} + k_1 \, f_{\ell u} \text{ (MPa)} \qquad (1)$$

Equation (1) expresses the influence of the lateral reinforcement confinement and by the FRP sheet, considering superposed effects when failure occurs. Chastre and Silva [5] suggest a value of k_1=5.29 for circular columns.

Having into account that for square columns there is the need to consider the influence of corners, equation (1) is adapted to the following expression:

$$f_{cc} = f_{c0} + k_1 \left(\frac{2R}{B}\right) f_{\ell u} \text{ (MPa)} \qquad (2)$$

Equation (2) was calibrated for CFRP with k_1=3.7 using the experimental tests (Fig. 8) presented in the previous section and testing data from several experimental studies [17, 22, 28, 29, 38-43].

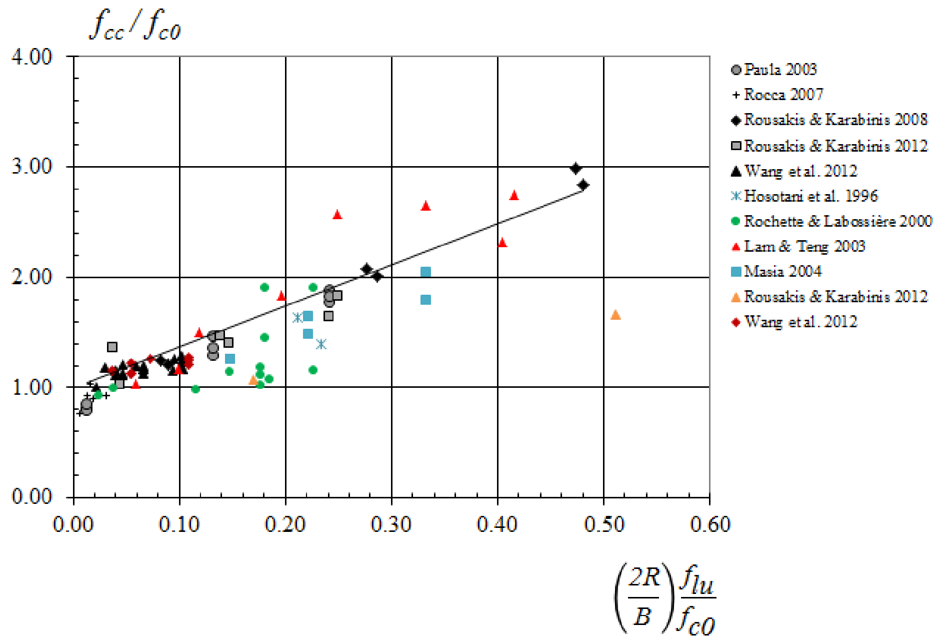

Fig. 8. Relationship between f_{cc}/f_{c0} and f_{lu}/f_{c0}. Square columns with cross-section dimension between 100x100 and 914x914 mm^2, confined with CFRP

Following the approach cited above, the lateral confinement, combining steel hoops and external FRP sheet, is defined by:

$$f_{\ell u} = f_{ju} + f_{shu} \text{ (MPa)} \quad (3)$$

$$f_{ju} = \frac{2t}{B} E_f \varepsilon_{\ell u} \quad (4)$$

$$f_{shu} = \frac{2A_{sw}}{d_w s} f_{sw} \quad (5)$$

where t represents the thickness; E_f the Young modulus and ε_{lu} the lateral ultimate strain of the FRP sheet and B is the diameter D of an equivalent circular cross-section as suggested by [43-45], which for square columns makes B=D. The steel cross section of the hoops is represented by A_{sw} and the diameter is d_w, assuming the same principle as B, and s the spacing between steel hoops. Since the tensile strength of the steel hoop f_{sw} is assumed constant after yielding, its relation with the lateral strain of the column ε_{lu} and the Young modulus E_s is considered until this point is reached:

$$f_{sw} = \begin{cases} E_s \times \dfrac{d_w}{B} \varepsilon_{\ell u} & \text{for} \quad \varepsilon_{\ell u} < \dfrac{B}{d_w} \varepsilon_y \\ f_y & \text{for} \quad \varepsilon_{\ell u} \geq \dfrac{B}{d_w} \varepsilon_y \end{cases} \quad (6)$$

It has been discussed and shown that lateral failure strain of the jacket ε_{lu} does not reach the failure strain of the CFRP ε_{fu} [18, 22, 45], mainly due to: non-uniform stress distribution in the FRP confinement due to internal concrete cracking; stress concentration on FRP due to localized buckling of longitudinal reinforcing steel; irregularities in the constitution of the FRP fabrics and multiaxial stress state due to bonding between concrete and the FRP. In view of these aspects Matthys et al. [46] proposed for circular columns the relation ε_{lu}=0.6ε_{fu}, which was also observed and highlighted by Realfonzo and Napoli [34] for lower and normal strength concrete (f_{co} ≤ 60MPa). These authors [34] also remarked slightly higher confinement efficiency (> 0.6) for lower confinement stiffness, though with high scatter, while Pellegrino and Modena [47] observed in their database analysis lower confinement efficiency when decreasing the confinement stiffness.

In the case of confined square columns, besides the aforementioned, the corner effect that makes that only part of the core is actually confined, should be particularly regarded. Yang et al. [48] studied the effect of corner radius on the strength of FRP laminates and on the distribution of the resulting radial stress on the substrate material. Accordingly and based on calibration through the tests presented by Paula [28] and Rocca [29], the following equation to obtain ε_{lu} is proposed:

$$\varepsilon_{lu} = 0.7\left(\frac{2R}{B}\right)^{0.23} \varepsilon_{fu} \qquad (7)$$

In circular columns the axial strain at peak load ε_{cc} is given by:

$$\varepsilon_{cc} = k_2^{'}\ \varepsilon_{c0}\left(\frac{f_{lu}}{f_{c0}}\right)^{0.7} \qquad (8)$$

where $k_2^{'}$=17.65 suggested by Chastre and Silva [5]

By regression of experimental data (Fig. 9) of square columns confined with CFRP and cross-section dimensions between 100x100 and 914x914 mm^2, Eq. (9) was calibrated with k_2=18.89.

$$\varepsilon_{cc} = k_2\ \varepsilon_{c0}\left(\frac{f_{lu}}{f_{c0}}\right) \qquad (9)$$

The axial strain at peak load of unconfined concrete ε_{c0} is adapted from Eurocode 2 [49]:

$$\varepsilon_{c0} = \frac{0.7}{1000}\left(f_{c0}\right)^{0.31} \qquad (10)$$

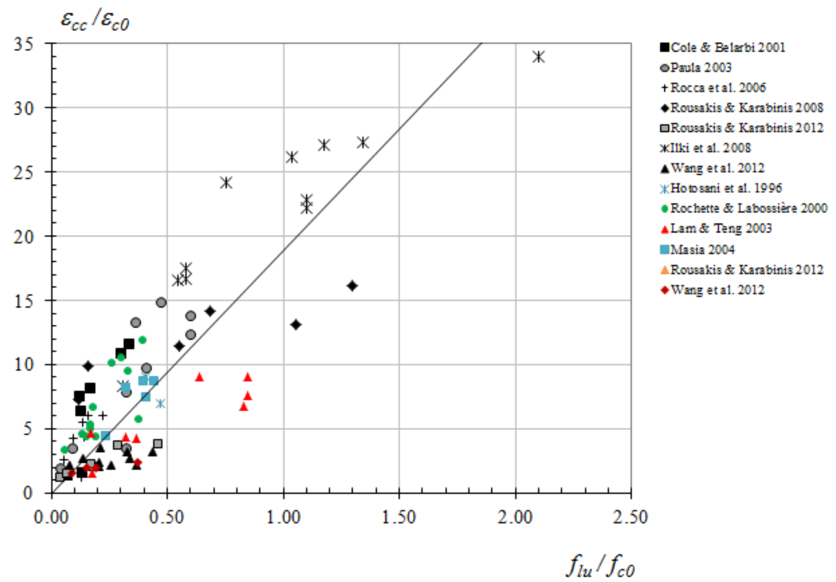

Fig. 9. Relationship between $\varepsilon_{cc}/\varepsilon_{c0}$ and f_{lu}/f_{c0}. Square columns with cross-section dimension between 100x100 and 914x914 mm^2, confined with CFRP

The maximum axial load N_{cc} in the RC column confined with CFRP sheet is obtained by:

$$N_{cc} = A_c f_{cc} + A_s f_s \qquad (11)$$

where A_c is the area of the columns' cross-section and A_s the longitudinal section of the reinforcing steel. The peak stress of the confined concrete f_{cc} is given by Eq. (1) and the tensile strength of the steel f_s is defined by:

$$f_s = \begin{cases} E_s \times \varepsilon_{cc} & \text{for} \quad \varepsilon_{cc} < \varepsilon_y \\ f_y & \text{for} \quad \varepsilon_{cc} \geq \varepsilon_y \end{cases} \qquad (12)$$

where ε_{cc} is the columns' axial strain at failure given by Eq. (9), E_s is the Young modulus, f_y the yield stress and ε_y is the matching strain of the longitudinal reinforcement.

4.2. Proposed Load–Strain Model for square RC columns confined with CFRP under compression

In the case of circular columns confined with CFRP the model proposed for the stress–strain curve is based on the relation, and corresponding parameters, represented in Fig. 10. For square columns this model may also be adopted though with significant changes for all the parameters involved and with particular differences concerning the trend of the branches after specimen's yielding.

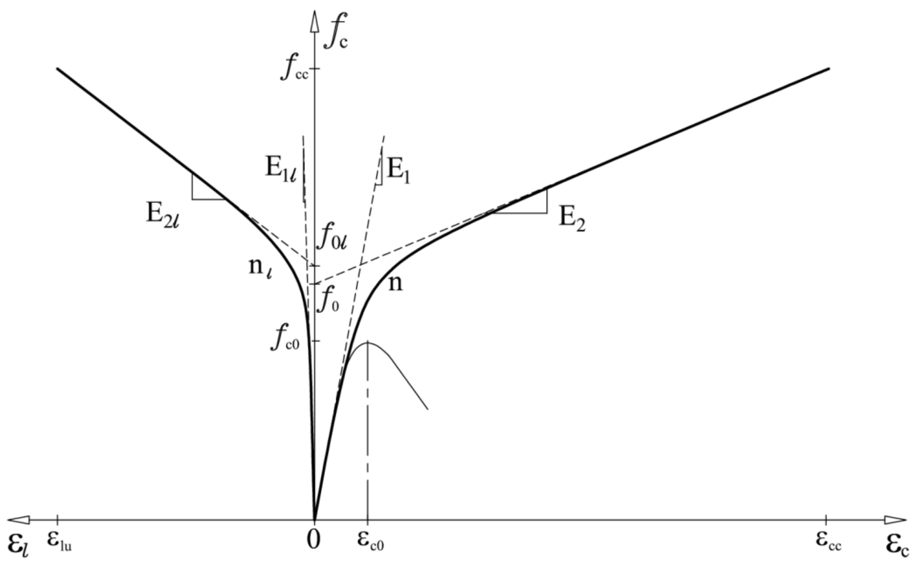

Fig. 10. Proposed model for axial compression behaviour of RC columns

The stress–axial strain relation is of two linear branches for concrete confined with CFRP and is based on Richard and Abbott's model [24] which includes four parameters: E_1, E_2, f_0 and n:

$$f_c = \frac{(E_1 - E_2)\varepsilon_c}{\left[1 + \left(\frac{(E_1 - E_2)\varepsilon_c}{f_0}\right)^n\right]^{\frac{1}{n}}} + E_2\varepsilon_c \leq f_{cc} \qquad (13)$$

Considering RC square columns with external CFRP sheets and the parameters calibrated based on existing testing results, the following equations are defined:

$$\begin{cases} E_1 = 3950\sqrt{f_{c0}} & \text{(a)} \\ E_2 = 510\left(\dfrac{2R}{B} f_{lu}\right)^{0.04} f_{c0}{}^{0.95} - 440 f_{c0} & \text{(b)} \\ f_0 = f_{c0} + 0.5\left(\dfrac{2R}{B}\right) f_{\ell u} & \text{(c)} \end{cases} \tag{14}$$

The same is used to represents the relation axial stress – lateral strain:,

$$f_c = \frac{(E_{1\ell} - E_{2\ell})\varepsilon_\ell}{\left[1 + \left(\dfrac{(E_{1\ell} - E_{2\ell})\varepsilon_\ell}{f_{0\ell}}\right)^{n_\ell}\right]^{\frac{1}{n_\ell}}} + E_{2\ell}\varepsilon_\ell \le f_{cc} \tag{15}$$

with

$$\begin{cases} E_{1\ell} = \dfrac{E_1}{\nu} & \text{(a)} \\ E_{2\ell} = 600\left(\dfrac{2R}{B} f_{\ell u}\right)^{0.11} (f_{c0})^{0.89} - 425 f_{c0} & \text{(b)} \\ f_{0\ell} = f_{c0} + 0.1\left(\dfrac{2R}{B}\right) f_{\ell u} & \text{(c)} \end{cases} \tag{16}$$

With regard to the axial stress – axial strain curve, the first slope of the curve is defined by Eq. (14a), similar to that of plain concrete as in [2], with f_{c0} and E_1 in MPa. The FRP confining sheet has a passive behaviour and is only activated when the lateral deformation reaches a point equivvalent to the maximum stress of the unconfined concrete. In view of this, the slope of the second branch, E_2 (Eq. 14b), is calibrated (Fig. 11) based on the tested behaviour of various square columns under axial compression and confined with CFRP with cross-section dimension between 150x150 to 914x914 mm^2. Accordingly, the stress value f_0 is estimated with resort to Eq 14c. Considering the experimental curves and those obtained from the proposed model (analytical), parameter n was assumed equal to 3.

Concerning the axial stress - lateral strain relation, the first slope of the curve E_{1l} depends on the concrete Poisson coefficient which is taken as 0.2 (Eq. 16a). Parameter n_l was assumed equal to 2. The modelling representation of the second slope E_{2l} (Eq. 16b) and the stress value of f_{0l} (Eq. 16c) are defined following the testing calibration as can be seen in Figs. 13 and 14.

The calculus method herein proposed to build analytically the stress–strain curves of concrete columns confined with CFRP under compression is simple and can be carried out building both curves, axial and lateral, separately knowing that the lateral strain failure ε_{lu} governs the end of both curves. The method of calculus is implemented through the next stages:

a) Establish the values of lateral strain ε_l from zero until the failure value ε_{lu} is reached, which is calculated using Eq. 7;
b) Use Eqs. 15 and 16a, 16b and 16c for the calculation of f_c and hence the stress-lateral strain curve. The end of the curve is set when the lateral strain ε_l reaches the lateral failure strain ε_{lu};
c) Use Eqs. 13 and 14a, 14b and 14c for the calculation of the axial stress-axial strain curve. The axial strain ε_c is set and its ultimate value ε_{cu} is attained when the axial stress f_c at lateral failure strain ε_{lu} is reached.

It should be noted that in the case in which the second slope is positive (E_2=positive value), the peak stress f_{cc} is equally the ultimate stress f_{cu}. As to those cases where the slope E_2 is negative, the ultimate stress f_{cu} is lower than the peak value f_{cc}, which makes the latter the main reference and priority from the point of view of design.

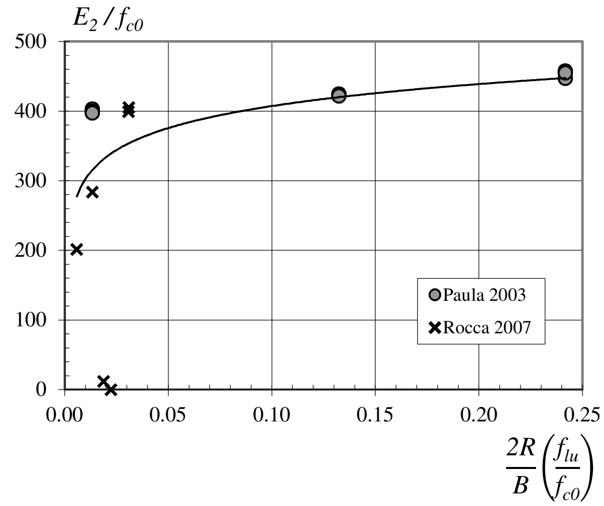

Fig. 11. Parameter E_2 - testing calibrations with RC square columns with cross-section dimension between 150x150 and 914x914 mm^2, confined with CFRP

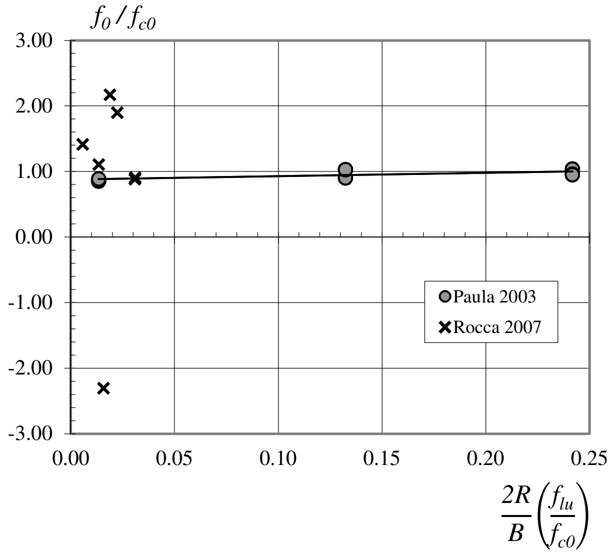

Fig. 12. Parameter f_0 - testing calibrations with RC square columns with cross-section dimension between 150x150 and 914x914 mm^2, confined with CFRP

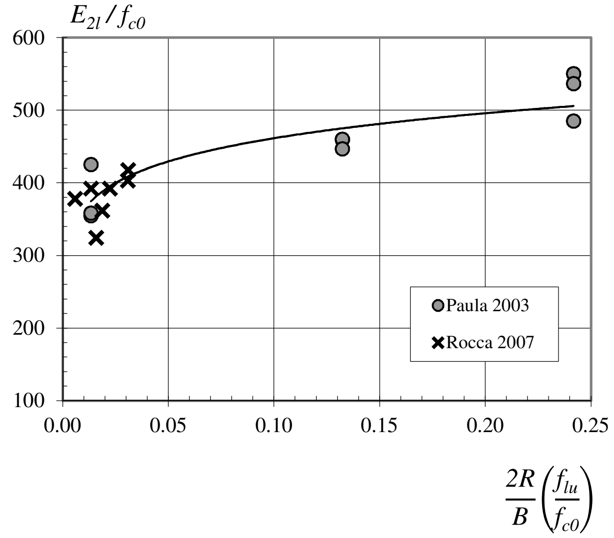

Fig. 13. Parameter E_{2l} - testing calibrations with RC square columns with cross-section dimension between 150x150 and 914x914 mm^2, confined with CFRP

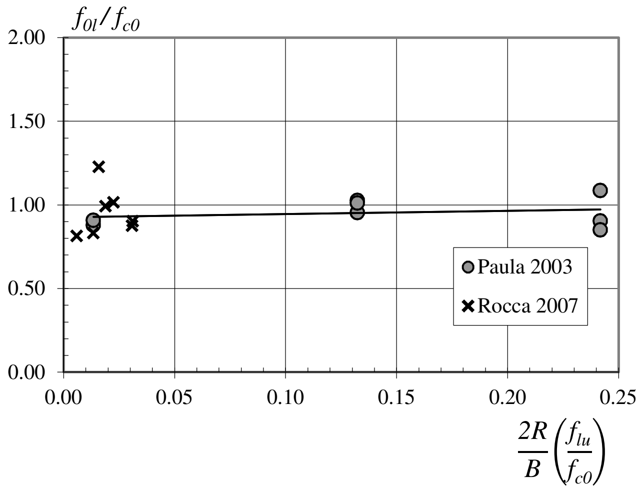

Fig. 14. Parameter f_{0l} - testing calibrations with RC square columns with cross-section dimension between 150x150 and 914x914 mm^2, confined with CFRP

In order to calculate the behaviour under uniaxial compression of square columns confined with CFRP and reinforced with longitudinal and transverse steel Eq. (16) can be used:

$$N_c = A_c f_c + A_s f_s \tag{17}$$

where N_c is the axial load, A_c is the total area of the cross-section of the column and A_s the total longitudinal reinforcement of the cross section. The stress f_c is obtained by Eqs. 13 to 17 and the steel stress f_s is defined by the ensuing equations:

$$f_s = \begin{cases} E_s \times \varepsilon_c & \text{for} \quad \varepsilon_c < \varepsilon_y \\ f_y & \text{for} \quad \varepsilon_c \geq \varepsilon_y \end{cases} \tag{18}$$

or

$$f_s \approx \begin{cases} E_s \times \varepsilon_\ell \times \nu & \text{for} \quad \varepsilon_\ell < \dfrac{\varepsilon_y}{\nu} \\ f_y & \text{for} \quad \varepsilon_\ell \geq \dfrac{\varepsilon_y}{\nu} \end{cases} \tag{19}$$

where ε_c is the axial strain and ε_l the lateral strain of the column, E_s is the reinforcing steel Young modulus, f_y and ε_y are the yield stress and strain of the longitudinal reinforcing steel.

4.3. Proposed model vs Experimental results

A set of 6 specimens of RC square columns with their testing results was chosen to serve as basis for the suitability analysis of the previously proposed equations.

This set includes CFRP confinement with 2, 5 and 8 layers, aspect ratios H/B of 2 and 5 and a CFRP volumetric ratio ρ_f of approximately 0.5 and 0.9. The input data used for the modelling of the columns' compression behaviour is presented in Tables 6 and 7.

Figs. 15 to 17 show the axial load–strain experimental curves (black lines) plotted along with the corresponding analytical curves (dashed lines) that were obtained based on the procedure proposed in section 4.2.

Table 6 - Geometrical section properties and detailing of columns' experimental curves of Paula [28] compared with the curves of the proposed analytical modelling.

Column	B (mm)	H/B	R/B	f_{c0} (MPa)	*MCR*	Long. steel reinf.	Transv. steel reinf.	E_f (GPa)	$t_{f\,CFRP}$ (mm)	$n_{f\,CFRP}$ (mm)	ε_{fu} (%)	ρ_L (%)	ρ_v (%)	ρ_f (%)
QR1C2	150	5.0	0	34.6	0.01	8Ø6	Ø3//100	217	0.176	2	1.76	1.00	0.11	0.94
QR2C2	151	5.0	0.132	34.6	0.13	8Ø6	Ø3//100	217	0.176	2	1.76	1.00	0.11	0.89
QR3C3	154	4.9	0.247	34.6	0.24	8Ø6	Ø3//100	217	0.176	2	1.76	1.00	0.11	0.85

Table 7 - Geometrical section properties and detailing of columns' experimental curves of Rocca [29] compared with the curves of the proposed analytical modelling.

Column	B (mm)	H/B	R/B	f_{c0} (MPa)	*MCR*	Long. steel reinf.	Transv. steel reinf.	E_f (GPa)	$t_{f\,CFRP}$ (mm)	$n_{f\,CFRP}$ (mm)	ε_{fu} (%)	ρ_L (%)	ρ_v (%)	ρ_f (%)
D2*	648	2.1	0.047	30.5	0.02	NA	NA	291	0.168	5 *	0.93	1.48	0.21	0.52
E3*	324	2.1	0.094	30.5	0.03	NA	NA	291	0.168	2.5 *	0.93	1.53	0.45	0.53
G2*	914	2.2	0.033	30.5	0.02	NA	NA	291	0.168	8 *	0.93	1.50	0.17	0.58

*obtained from the volumetric ratio of CFRP confinement ρ_f; NA – not available

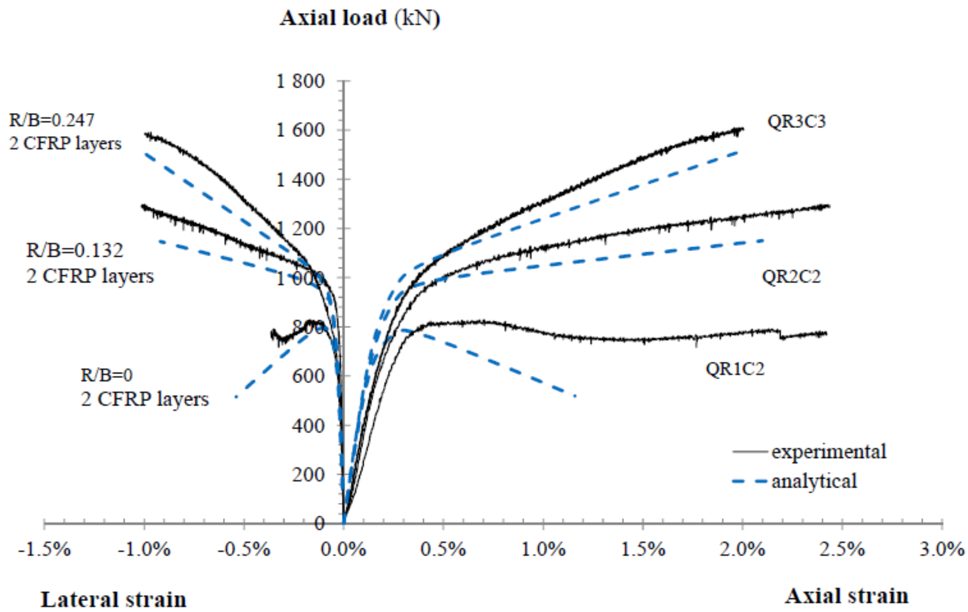

Fig. 15. RC square columns 150x150mm^2 confined with CFRP: Experimental vs. Analytical behaviour. Experimental data obtained from Paula [28]

The experimental work carried out by Paula [28] aimed to study the corner effect on the behaviour of RC square columns under axial loading. The enhancement is evident the rounder the corners are. The implementation of the proposed model for the simulation of this behaviour (analytical curves: QR1C2; QR2C2 and QR3C3) follows the same trend as the experimental results (Fig. 15). As seen from Fig. 15 the overall results show good agreement for all columns, although for column QR2C2 is the axial strength N_{cc} is slightly underestimated. As regards deformation, the results of ultimate axial strain ε_{cu} are underestimated except for column QR3C3, while column QR1C2 overestimates the ultimate lateral strain ε_{lu}.

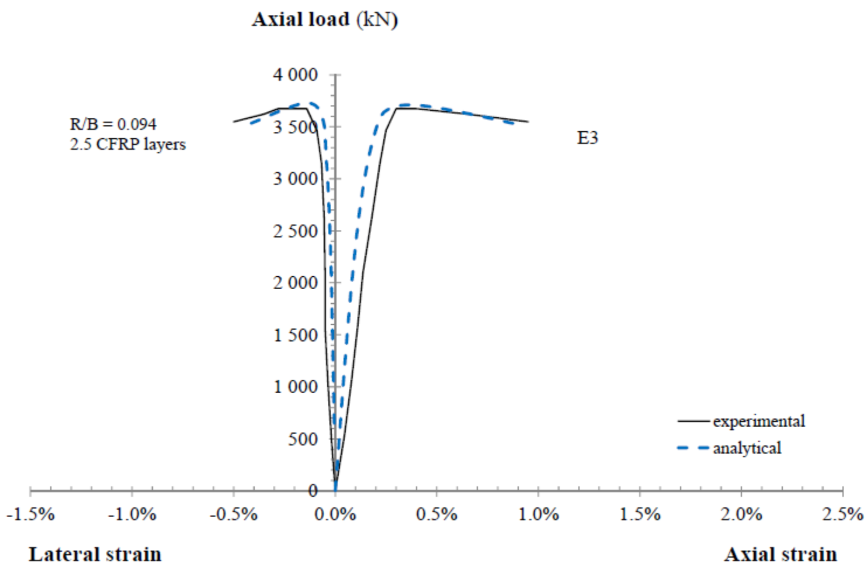

Fig. 16. RC square columns 324x324 mm^2 confined with CFRP: Experimental vs. Analytical behaviour. Experimental data obtained from Rocca [29]

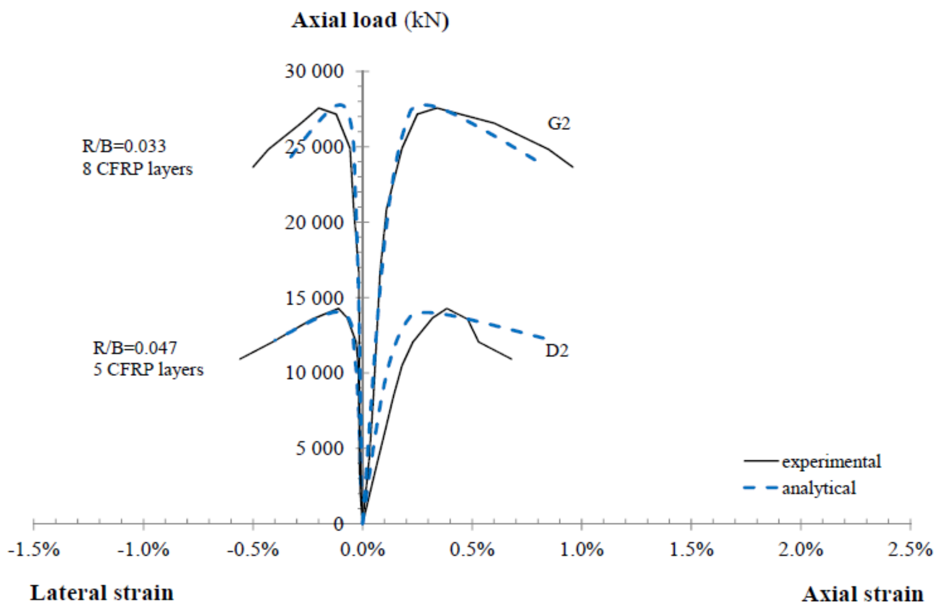

Fig. 17. RC square columns 648x648 and 914x914 mm^{2}confined with CFRP: Experimental vs. Analytical behaviour. Experimental data obtained from Rocca [29]

As regards the experimental work by Rocca [29], the tested columns have relevant differences concerning side lengths, which cover commonly used dimensions of full scale columns. When experimental and analytical strength values *Ncc* are compared it can been seen that differences are of little significance. As to deformation, the results of ultimate axial strain ε_{cu} are underestimated except for column D2. As to lateral strain ε_{lu} the results concerning columns E3 and G2 are underestimated. In the specific case of column E3, for the second branch of both axial and lateral curves the superposition is almost complete.

The presented tested columns show second branches with both ascending and descending slopes. Despite some of the differences between experimental and analytical results, the predicted load-strain relations are still, globally, in agreement with the experimental results. The comparison results in Figs 15 to 17 validate thus the application of the proposed model for columns with dimensions ranging from small to full scale sizes. The analytical results shown in Fig. 18 express how wide is the range of application of the proposed model, concerning the dimension of columns, with reliable results.

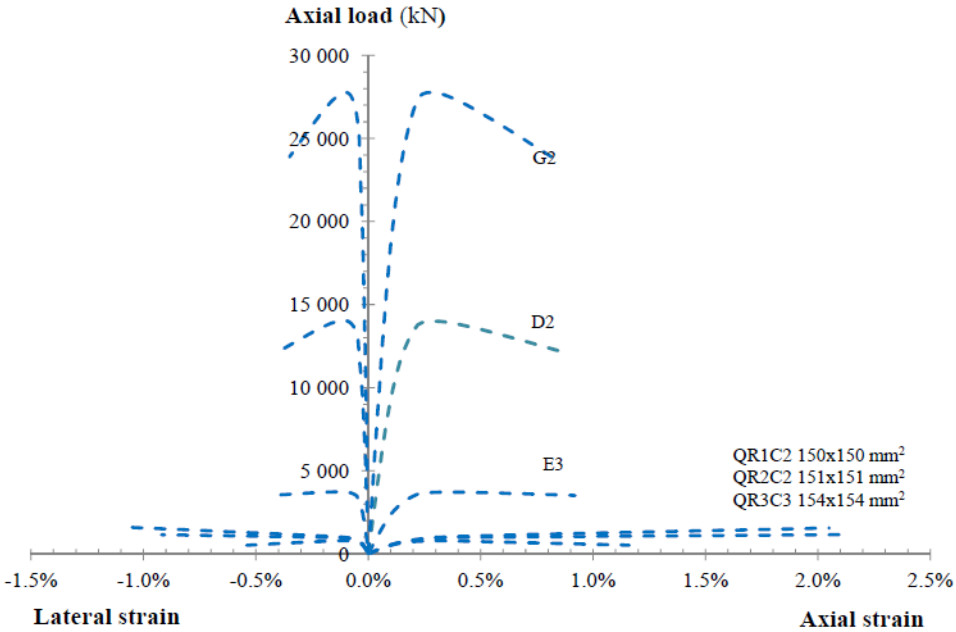

Fig. 18. RC square columns confined with CFRP: cross-section 150x150 to 914x914 mm^2. Analytical behaviour based on the proposed model.

5. Final remarks

In this work a set of experimental results of various researchers was used to create a practical analytical model to estimate the behaviour of RC square columns confined with CFRP under axial compression. Most of the proposed equations rely on the experimental results by Paula [28] and Rocca [29] of which 6 columns were chosen to verify the validation of the proposed model. The experimental results by Paula [28] and Rocca [29] show that the geometry of the section has a substantial impact on the behaviour of columns strengthened with FRP. The experimental results clearly show that columns with circular cross-section have better performance – higher strength and axial strain – when compared to square columns. For the latter, there is an evident influence of the corner ratio *R/B*, especially if regarded that the higher this parameter is the greater axial strength N_{cc} gets. Moreover, if the *R/B* parameter increases, the slope of the second branch E_2 may vary from negative (descending slope) to positive and higher values (ascending slope). Considering the axial load – lateral strain behaviour and specifically the ultimate lateral strain ε_{lu}, there is no significant difference between circular columns and square columns with round corners, while for columns with sharp edges (R/B≈0) the second branch is shorter. Additionally, it seems that side length has no significant influence itself on columns' performance but rather the corner ratio and the confinement ratio.

The modelling procedure herein proposed is suitable to a simple method for the design of RC square confined with CFRP subjected to axial compression. Amongst other parameters, it considers the contribution of both longitudinal and transversal reinforcing steel on columns' structural performance.

The proposed equations also consider explicitly the effect of corner radius on columns' confining action which, according to the experimental results of the tested columns, has a significant influence on their overall behaviour.

The model proves to be reliable for square columns from 150 to 914 mm side dimension with aspect ratios H/B between 2 and 5 and CFRP strengthening ratios of 0.2% and 0.9%. The analytical results, based on the proposed model, are in general good agreement with the curves obtained from experimental tests.

References

[1] Richart FE, Brandtzaeg A, Brown RL. A study of the failure of concrete under combined compressive stresses. Bulletin No. 185, University of Illinois Engineering Experimental Station, Champaign, Ill; 1928.

[2] Ahmad SH, Shah SP. Stress–strain curves of concrete confined by spiral reinforcement. ACI Structural Journal 1982;79(6):484-90.

[3] Fardis, MN, Khalili H. FRP-Encased Concrete as Structural Material. Magazine of Concrete Research (Wexham Springs), 1982;34(121): p. 191-202.

[4] Mander JB, Priestley MJN, Park R. Theoretical stress-strain model for confined concrete. J Struct Eng 1988;114(8):1804-26.

[5] Chastre C, Silva MAG. Monotonic axial behavior and modelling of RC circular columns confined with CFRP. Engineering Structures 2012;32(8):2268-2277.

[6] Marques PF, Chastre C. Performance analysis of load-strain models for circular columns confined with FRP composites. Composite Structures 2010;94(11):3115-31.

[7] De Lorenzis L, Tepfers R. (2003). "Comparative Study of Models on Confinement of Concrete Cylinders with Fiber-Reinforced Polymer Composites." ASCE Journal of Composites for Construction, 7(3): 219-234.

[8] Rousakis, T.C., Karabinis, A.I., Kiousis, P.D., Tepfers, R., (2008) Analytical modelling of plastic behaviour of uniformly FRP confined concrete members, Composites Part B: Engineering 39 (7-8) , pp. 1104-1113

[9] Rousakis TC, Rakitzis TD, Karabinis AI. Design-Oriented Strength Model for FRP-Confined Concrete Members. Journal of Composites for Construction Dec 2012, Vol. 16, No. 6, pp. 615-625

[10] Dai Jian-Guo, Bai Yu-Lei, Teng J. G. "Behavior and Modeling of Concrete Confined with FRP Composites of Large Deformability", Journal of Composites for Construction, 2011, Vol. 15, No. 6, pp. 963- 973.

[11] Mirmiran A, Shahawy M. Dilation characteristics of confined concrete. Mech Cohes-Frict Mater 1997;2(3):237-49.

[12] Grassl P. Modelling of dilation of concrete and its effect in triaxial compression. Finite Elem Anal Des 2004;40(9-10):1021-33.

[13] Spoelstra M, Monti G. FRP-confined concrete model. J Compos Constr 1999;3(3).

[14] Rousakis TC, Karabinis AI, Kiousis PD. FRP-confined concrete members: Axial compression experiments and plasticity modelling. Eng Struc, 2007;29(7): 1343-1353.

[15] Saenz, N, Pantelides CP. Strain-Based Confinement Model for FRP-Confined Concrete. Journal of Structural Engineering, 2007;133(6): p. 825-833.

[16] Ilki A, Peker O, Karamuk E,.Demir C, Kumbasar N. FRP retrofit of low and medium strength circular and rectangular reinforced concrete columns. Journ Mater Civil Eng 2008;20(2): 169-188.

[17] Rochette P, Labossière P. Axial testing of rectangular column models confined with composites. Journal Composites Construction 2000; 4(3): 129-136

[18] Samaan M., Mirmiran A, Shahawy M. Model of concrete confined by fiber composites. Journal of Structural Engineering 1998;124(9): 1025-1031.

[19] Manfredi G, Realfonzo R. Models of concrete confined by fiber composites, FRPRCS-5, Thomas Telford, London, 2001:865-874

[20] Wang YC, Restrepo JI. Investigation of concentrically loaded reinforced concrete columns confined with glass fiber-reinforced polymer jackets. ACI Structural Journal 2001;98(3): 377-385.

[21] Campione G, Miraglia N. Strength and strain capacities of concrete compression members reinforced with FRP. Cement & Concrete Composites 2003;25(1): 31-41.

[22] Lam L, Teng JG, Design-Oriented Stress-Strain Model for FRP-Confined Concrete in Rectangular Columns. Journal of Reinforced Plastics and Composites, 2003. 22(13): p. 1149-1186.

[23] Lee C. Modeling of FRP-jacketed RC columns subject to combined axial and lateral loads, University of San Diego, California, PhD Thesis 2006.

[24] Richard RM, Abbott BJ. Versatile Elastic-Plastic Stress-Strain Formula. Journal of the Engineering Mechanics Division, 1975. 101(4): p. 511-515.

[25] Pantazopoulou SJ, Mills RH, Microstructural Aspects of the Mechanical Response of Plain Concrete. ACI Materials Journal, 1995. 92(M62): p. 605-616.

[26] Popovics S. A numerical approach to the complete stress-strain curve of concrete. Cement and Concrete Research, 1973. 3(5): 583-599.

[27] Saatcioglu, M. and S. R. Razvi. Strength and Ductility of Confined Concrete. Journal of Structural Engineering 1992; 118(6): 1590-1607.

[28] Paula R. Influência da geometria das secções no confinamento de pilares de betão armado com compósitos de CFRP. Inst Sup Técnico/UTL, Lisboa, MSc Dissert 2003.

[29] Rocca S. Experimental and analytical evaluation of FRP-confined large size reinforced concrete columns. University of Missouri-Rolla, PhD Thesis 2007.

[30] ASTM C39/C39M - 01 Standard Test Method for Compressive Strength of Cylindrical Concrete Specimens, 2001.

[31] ASTM D3039/D3039 - 00. Standard test method for tensile properties of polymer matrix composite materials, 2000.

[32] NP EN 10002-1. Tensile Testing of Metallic Materials. IPQ, Lisbon, 1990.

[33] *fib* bulletin 14. Externally bonded FRP reinforcement for RC structures. Lausanne; 2001.

[34] R. Realfonzo, A. Napoli, Concrete confined by FRP systems: Confinement efficiency and design strength models, Composites: Part B 42 (2011) 736-755

[35] Pessiki S, Harries KA, Kestner JT, Sause R, Ricles JM. Axial behavior of reinforced concrete columns confined with FRP jackets. J Compos Constr. 2001;5(4):237-45.

[36] Lam L, Teng JG. Ultimate condition of fiber reinforced polymer-confined concrete. J Compos Constr. 2004;8(6):539-48.

[37] Mirmiran A, Shahawy M, Samaan M, Echary HE. Mastrapa JC, Pico O. Effect of Column Parameters on FRP-confined Concrete. Journal of Composites for Construction, 1998; 2(4):175-184.

[38] Cole C, Belarbi A. FRP jacketed reinforced concrete columns. Report CIES 99-13. University of Missouri-Rolla, 2001.

[39] Rousakis TC, Karabinis AI. Substandard reinforced concrete members subjected to compression: FRP confining effects. Materials and Structures 2008;41(9): 1595-1611.

[40] Rousakis TC, Karabinis AI. Adequately FRP confined reinforced concrete columns under axial compressive monotonic or cyclic loading. Materials and Structures 2012;45(7): 957-975.

[41] Wang Z, Wang D, Smith TS, Lu D. CFRP-Confined square RC columns. I: Experimental investigation. Journal Composites Construction, 2012; 16(2):150-160.

[42] Hosotani M, Kawashima K, Hoshikuma J. Seismic Retrofit of Reinforced Concrete Bridge Piers by Carbon Fiber Sheets. Proceedings of the Third U.S.-Japan Workshop on Seismic Retrofit of Bridges, December 10 and11, 1996; pp. 217-242.

[43] Masia JA, Gale TN, Shrive NG. Size effects in Axially Loaded Square-Section Concrete Prisms Strengthened Using Carbon Fiber Reinforced Polymer Wrapping. Canadian Journal of Civil Engineering 2004; 31:1-13.

[44] ACI 440.2R-02. Guide for the Design and Construction of Externally Bonded FRP Systems for Strengthening of Concrete Structures. American Concrete Institute, 2002, Farmington Hills, MI, USA.

[45] Matthys S. Structural Behaviour and Design of Concrete Members Strengthened with Externally Bonded FRP, in Faculty of Applied Sciences, Department of Structural Engineering. 2000, DSc, Ghent University.

[46] Matthys S, Toutanji H, Taerwe L. Stress–Strain Behavior of Large-Scale Circular Columns Confined with FRP Composites. Journal of Structural Engineering 2006;132(1), 123-133.

[47] Pellegrino C, Modena C. Analytical model for FRP confinement of concrete columns with and without internal steel reinforcement. J Compos Constr. 2010;14(6):693-705;

[48] Yang X, Wei J, Nanni A, Dharani LR. Shape effect on the performance of carbon fiber reinforced polymer wraps. Journal of Composites for Construction 2004:8(5);444-451.

[49] EN 1992-1-1. Eurocode 2. Design of concrete structures. Part 1-1: general rules and rules for buildings. Brussels: CEN; 2004.